Ultralow PM and AM Noise Generation With an Ensemble of Phase-Coherent Oscillators

Archita Hati, *Member, IEEE*, Marco Pomponio, and Craig W. Nelson, *Member, IEEE*

***Abstract*—This article investigates the performance of an array of multiple phase-coherent power-combined oscillators (PPOs) in terms of phase modulation (PM) noise and amplitude modulation (AM) noise. The array consists of six individual oscillator modules that generate three distinct frequencies: 10, 100 MHz, and 1 GHz. By meticulously aligning the phases, we observed a notable improvement of approximately 7.8 dB in the white frequency region for the power-combined signal's AM and PM noise. This closely matches the theoretical value of $10\log_{10}(k)$ dB, where k is the total number of oscillators. The enhancement arises from the fact that when multiple sources are combined, the power of each source adds coherently, while the random noise adds noncoherently. Our experiments resulted in single-sideband (SSB) white phase noise levels of −182, −191, and −168 dBc/Hz for 10, 100 MHz, and 1 GHz, respectively. The corresponding white AM noise levels are approximately −191, −194, and −182 dBc/Hz. Notably, these noise levels represent some of the lowest ever reported at these frequencies. However, the AM noise results for frequencies close to the carrier do not achieve the theoretical 7.8-dB improvement due to PM-to-AM conversion caused by imperfect phase alignment of the individual summed signals. Furthermore, we discuss the use of carrier-suppressed noise measurement and propose a novel, straightforward technique for optimizing phase alignment to minimize PM-to-AM and AM-to-PM conversion in phase-coherent oscillator arrays.**

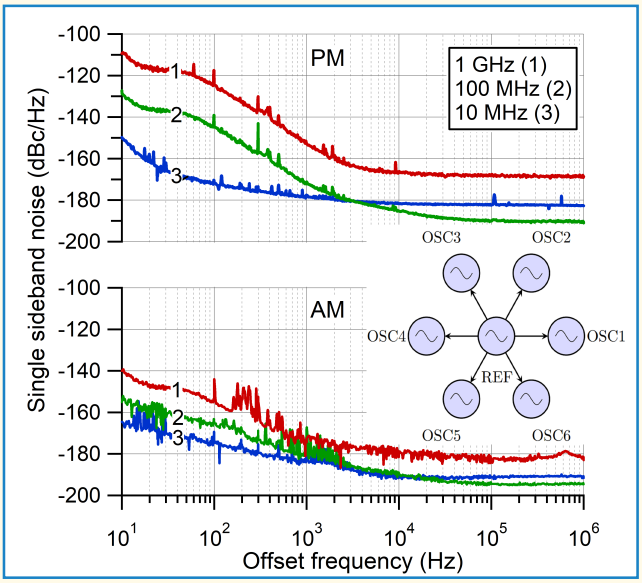

***Index Terms*— AM-to-PM conversion, amplitude modulation (AM) noise, Armstrong modulator, phase modulation (PM) noise, phase-coherent oscillators, phase-locked loop (PLL), PM-to-AM conversion.**

I. Introduction

LOW phase modulation (PM) and amplitude modulation (AM) noise oscillators are essential in a wide range of applications. For instance, radar systems rely on low phase noise sources to accurately detect and measure small and fast objects [1], [2], [3]. In wireless communication systems, low phase noise is also critical for achieving high signal quality and data transfer rates [4], [5], and in medical imaging, it sets the ultimate resolution [6], [7], [8], [9]. Similarly, in scientific research, low phase noise sources are used in high-resolution spectroscopy, precision timing, and frequency metrology [10]. In addition, low phase noise sources and circuits are crucial for digital signal processing, instrumentation, and audio applications where noise and distortion can degrade performance [11]. Low AM noise sources are important as well, especially for phase noise metrology for minimizing the impact of AM-to-PM conversion in phase detectors [12]. Overall, any application that requires spectral purity can benefit from low phase and amplitude noise sources.

Often noise levels of oscillators are above the required specifications for a system, and implementing noise reduction becomes necessary. There are various well-known methods that can be used to improve the phase noise of oscillators. The techniques of feedback and feedforward are commonly used to reduce the noise in oscillators and two-port devices, such as amplifiers [13], [14], [15], [16]. Furthermore, strategies that use correlation between PM and AM noise of oscillator loop components have shown to reduce phase noise of oscillators [17], [18], [19]. By combining the outputs of two or more independent oscillators that are phase-locked or

Manuscript received 14 August 2023; accepted 7 December 2023. Date of publication 12 December 2023; date of current version 26 January 2024. *(Corresponding author: Archita Hati.)*

Archita Hati and Craig W. Nelson are with the Time and Frequency Division, National Institute of Standards and Technology, Boulder, CO 80305 USA (e-mail: archita.hati@nist.gov; nelson@nist.gov).

Marco Pomponio is with the Time and Frequency Division, National Institute of Standards and Technology, Boulder, CO 80305 USA, and also with the Department of Electrical, Computer, and Energy Engineering, University of Colorado, Boulder, CO 80309 USA (e-mail: marco.pomponio@nist.gov).

Digital Object Identifier 10.1109/TUFFC.2023.3341726

Highlights

- **This paper demonstrates near-optimal PM and AM noise reduction via an array of phase-coherent oscillators. It also discusses a novel digital Armstrong modulator for minimizing PM↔AM noise conversions.**
- **We achieved white PM noise levels of −182, −191, and −168 dBc/Hz for 10, 100 MHz, and 1 GHz, respectively. The corresponding white AM noise levels are approximately −191, −194, and −182 dBc/Hz.**
- **The proposed oscillators with high spectral purity and the new digital modulator possess great potential in precision phase noise metrology and applications requiring ultralow phase noise.**

injection-locked to each other, it is possible to reduce the phase and amplitude noise of the combined output signal. However, the phase noise reduction due to the coherent addition of the signals will only be observed at offset frequencies outside the phase-locked loop (PLL) bandwidth (BW). Extensive theoretical work and experimental work on mutually synchronized oscillator systems for various coupling topologies are presented in the literature [20], [21], [22], [23]. In previous work, the PM noise reduction in phase-coherent oscillators is discussed; however, AM-to-PM or PM-to-AM noise conversion has been mostly ignored.

In this article, we examine the PM and AM noise performance of an array of six PPOs when arranged in a star configuration where all the oscillators are phase-locked to a common reference. This work originated from a different project that required the development of six low-noise, multifrequency oscillators with phase-lockable 10-MHz reference and a phase shifter at the output. The availability of six such oscillators with all the required elements needed to build a high-performance phase-coherent power-combined array provided an ideal and unique opportunity to perform this experiment.

II. PM and AM Noise of Phase-Coherent Array of Oscillators

When the outputs of two or more independent but synchronized oscillators are combined, it is possible to reduce the contribution of uncorrelated phase and amplitude noise from individual oscillators to the total combined output signal. This approach necessitates phase-locking of the individual oscillators. To elucidate the theory of a phase-coherent array of oscillators, we define a set of k equations describing the output voltage of oscillators with independent noise processes as

$$v_i(t) = A\big[1 + \alpha_i(t) + j\varphi_i(t)\big]e^{j\omega t}, \quad \text{where } i = 1, 2, \ldots, k. \tag{1}$$

Here, A and ω denote the amplitude and angular frequency, respectively. The random variables α_i, and φ_i represent fractional amplitude fluctuations and phase fluctuations for each individual signal, respectively. In this analysis, α_i, and φ_i will take into account the contributions of both the parametric and additive noise processes. A complex signal is used to represent the oscillators, and this is done solely to simplify the analysis and equations. In (1), we assume that the noise modulations are small. The output of the Wilkinson power combiner, $v_\Sigma(t)$, can be written as

$$v_\Sigma(t) = \frac{-j}{\sqrt{k}}\left[A\left(k + \sum_{i=1}^{k}\alpha_i(t) + j\sum_{i=1}^{k}\varphi_i(t)\right)e^{j\omega t}\right]. \tag{2}$$

Considering that the correlated signal amplitude adds linearly, while uncorrelated noise variables add as their expected powers, the power spectral densities (PSDs) of the resultant signal can be expressed as

$$S_{\alpha_\Sigma}(f) = \frac{S_\alpha(f)}{k}$$
$$S_{\varphi_\Sigma}(f) = \frac{S_\varphi(f)}{k}. \tag{3}$$

Here, S_{α_Σ}, S_{φ_Σ}, and S_α, S_φ denote the double-sideband (DSB) AM noise, PM noise of the combined signals, and AM noise, PM noise of the individual oscillators, respectively. For simplicity, we assume that $S_\alpha = S_{\alpha_i}$ and $S_\varphi = S_{\varphi_i}$ for all k signals. Equation (3) illustrates that the AM noise and PM noise experience a reduction factor of k in the combined output compared with a single output.

To achieve this noise reduction, the k input signals to the power combiner must exhibit the same average frequency and be perfectly phase-aligned. This can be accomplished using PLLs and additional phase shifters for fine adjustment. Various synchronization topologies are possible [22], but in this article, we solely investigate the "star" configuration depicted in the abstract and in Fig. 1. For our proposed phase-locked star configuration, the PM noise reduction given in (3) occurs only for offset frequencies greater than the PLL BW since all k oscillators are correlated inside the BW. On the other hand, the phase-locking does not affect the AM noise reduction inside the BW.

III. Experimental Setup of Phase-Coherent Array of Oscillators

For the PPO configuration, we used a total of six oscillators, phase-locked to a common 10-MHz reference, as depicted in Fig. 1. Each pair of three oscillators was first power-summed in a three-way power combiner, and the final composite signal was derived from the Σ-port of the 180° hybrid. The delta-port of the hybrid was primarily used for the PM and AM noise measurements using carrier suppression (CS) technique [11], [24], [25].

In power-summed oscillators, precise phase alignment among the individual input oscillators is crucial for achieving optimal noise at the output. Any deviation from the perfect phase alignment can result in the projection of PM noise into the AM quadrant and AM noise into the PM quadrant,

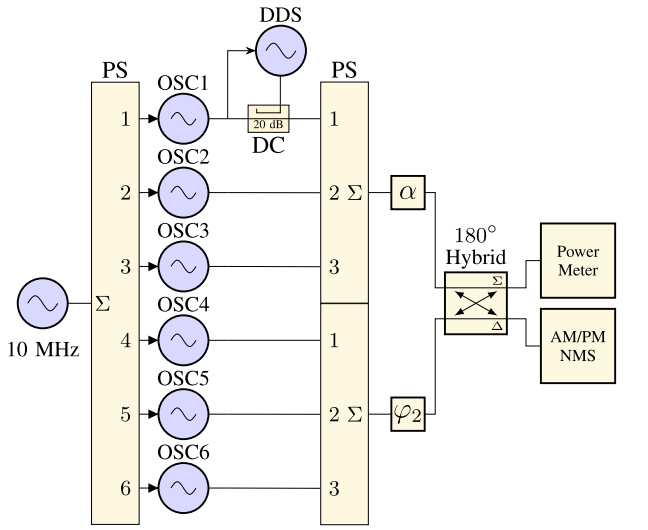

Fig. 1. Block diagram of phase-coherent array of oscillators. DDS—direct digital synthesizer; DC—directional coupler; NMS—noise measurement system; OSC—oscillator; PS—power splitter/combiner; α—attenuator; φ_2—phase shifter.

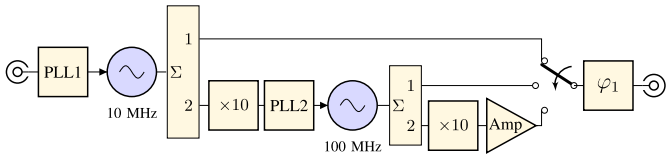

Fig. 2. Block diagram of multifrequency oscillators (OSC1–OSC6) used in the phase-coherent array configuration in Fig. 1. A coaxial relay is used to select one of the three frequencies at 10, 100 MHz, and 1 GHz.

resulting in a deviation from the ideal noise reduction effect described in (3). To address this, we introduced a 20-dB directional coupler (DC) at the output of oscillator #1 to inject a PM alignment signal. A phase shifter (φ_2) was inserted to adjust the AM-to-PM and PM-to-AM conversion at the outputs of the hybrid, and a fixed attenuator (α) was used to adjust the level of CS. The CS method, the influence of PM-to-AM conversion, and the alignment procedure will be discussed in detail in Section IV.

Each oscillator in the array was a commercial multifrequency oven-controlled crystal oscillator (OCXO) module (NEL, Model# O-CMR058IS-N-E-S-L−10 MHz/100 MHz/1000 MHz), capable of generating frequencies of 10, 100 MHz, and 1 GHz. The individual oscillator module and its associated components are illustrated in Fig. 2. To ensure stable operation, we designed a custom PLL (PLL1) that locked the oscillator module to a 10-MHz external reference signal. In addition, an external amplifier (Amp) was incorporated to amplify the 1-GHz output signal. The amplifier operated within a range of 1–2-dB compression. To select the desired frequency, we used a coaxial switch. The output of the switch was routed through a phase shifter capable of providing 90° phase shift at 1 GHz. This phase shifter provided the fine phase adjustment needed to achieve desired CS.

IV. Measurement Technique

To enhance the sensitivity of our PM and AM noise measurements, we used a CS technique. This technique involves suppressing the output carrier signal at the Δ-port of the 180° hybrid, accomplished by adjusting the phase shifter and fixed attenuator as illustrated in Fig. 1. The suppressed signal was then connected to the Rohde and Schwarz FSWP50 noise analyzer, allowing simultaneous measurement of absolute AM and PM noise. Typically, when using high levels of CS, an amplifier is required to restore the carrier power to the minimum level necessary for the measurement system. However, to avoid introducing additional noise contributions from an amplifier, we deliberately chose not to use one.

At offset frequencies far from the carrier, the FSWP50 noise analyzer can measure the single-sideband (SSB) AM and PM noise as low as the thermal signal-to-noise limit $(k_B T)/(2P_0)$. Here, k_B is Boltzmann's constant, T is the temperature in Kelvin, and P_0 is the carrier power at the input of the noise analyzer. The newer firmware update for the FSWP50 implements a software correction that prevents cross-spectral collapse due to the anti-correlation effect caused by the thermal noise from the common-mode power-splitter (PS) in the noise analyzer [26], [27], [28]. The close-to-the carrier AM noise floor of the FSWP50 is significantly higher than the AM noise of the oscillators being measured. For example, the instrument AM noise floor at 10-Hz offset ranges between −130 and −135 dBc/Hz for a cross correlation factor of 1000 for all the three frequencies under considerations. Therefore, a CS approach was required for AM noise measurements. For the same correlation factor, the PM noise floor of the analyzer at a 10-Hz offset for carrier frequencies of 10, 100 MHz, and 1 GHz is approximately −145, −131, and −111 dBc/Hz, respectively. Unlike AM noise measurements, the analyzer was able to measure the close-to-the-carrier PM of the oscillators at the Σ-port. However, CS measurement technique at the Δ-port enabled shorter measurement times and noise plots exhibited less statistical variations. Nonetheless, the direct and CS measurements were also compared to validate the CS noise enhancement factors, as discussed in Section IV-B.

A. PM-to-AM Conversion

Commonly, the AM noise in oscillators is lower than the PM noise near the carrier frequency. This characteristic holds true for the oscillators used in our experiment across most offset frequencies, making AM-to-PM conversion negligible. However, at near-carrier offsets, the PM noise surpasses the AM noise by several orders of magnitude. Due to imperfect phase alignment, the dominant conversion effect that we observed in our proposed method was PM-to-AM. This conversion affected both the composite signal at the Σ-port and the carrier-suppressed signal at the Δ-port of the hybrid.

To model the effect of these conversions in our k-PPO configuration (k is even), we write the output of a pair of $k/2$-way power combiners as follows:

$$v_1(t) = \frac{-j}{\sqrt{k/2}} \sum_{i=1}^{\frac{k}{2}} \left[A(1 + \alpha_i(t) + j\varphi_i(t)) e^{j\omega t} \right] \tag{4a}$$

$$v_2(t) = \frac{-j}{\sqrt{k/2}} \sum_{i=\frac{k}{2}+1}^{k} \left[A(1 + \alpha_i(t) + j\varphi_i(t)) e^{j(\omega t+\theta)} \right]. \tag{4b}$$

To simplify, we assume all k signals have the same amplitude, and the $k/2$ signals in each pair have the same phase. The signals at the Σ- and Δ-ports of the 180° hybrid are

$$v_\Sigma(t) = \frac{-j}{\sqrt{2}}[v_1(t) + \rho v_2(t)] \tag{5a}$$

$$v_\Delta(t) = \frac{-j}{\sqrt{2}}[v_1(t) - \rho v_2(t)]. \tag{5b}$$

Here, ρ represents an amplitude scaling factor, and θ denotes the phase shift between $v_1(t)$ and $v_2(t)$. Using a first-order Taylor expansion around $\theta = 0$ with θ' representing $\theta \ll 1$, for the Σ-port, we rewrite (5a) as

$$v_\Sigma(t) = \frac{A\sqrt{k}(1+\rho)}{2}\left[1 + \alpha_\Sigma(t) + j\varphi_\Sigma(t)\right]e^{j\left(\omega t + \frac{\rho\theta'}{\rho+1} + \pi\right)} \tag{6a}$$

$$\alpha_\Sigma(t) = \frac{2}{k(1+\rho)} \times \sum_{i=1}^{\frac{k}{2}}\left[\alpha_i(t) + \rho\alpha_{\frac{k}{2}+i}(t) + \frac{\rho\theta'}{\rho+1}\left(\varphi_i(t) - \varphi_{\frac{k}{2}+i}(t)\right)\right] \tag{6b}$$

$$\varphi_\Sigma(t) = \frac{2}{k(1+\rho)} \times \sum_{i=1}^{\frac{k}{2}}\left[\varphi_i(t) + \rho\varphi_{\frac{k}{2}+i}(t) + \frac{\rho\theta'}{\rho+1}\left(-\alpha_i(t) + \alpha_{\frac{k}{2}+i}(t)\right)\right]. \tag{6c}$$

Similarly, for the Δ-port, we can rewrite (5b) as

$$v_\Delta(t) = \frac{A\sqrt{k}(1-\rho)}{2}\left[1 + \alpha_\Delta(t) + j\varphi_\Delta(t)\right]e^{j\left(\omega t + \frac{\rho\theta'}{\rho-1} + \pi\right)} \tag{7a}$$

$$\alpha_\Delta(t) = \frac{2}{k(1-\rho)}\sum_{i=1}^{\frac{k}{2}}\left[\alpha_i(t) - \rho\alpha_{\frac{k}{2}+i}(t) + \frac{\rho\theta'}{\rho-1} \times \left(\varphi_i(t) - \varphi_{\frac{k}{2}+i}(t)\right)\right] \tag{7b}$$

$$\varphi_\Delta(t) = \frac{2}{k(1-\rho)}\sum_{i=1}^{\frac{k}{2}}\left[\varphi_i(t) - \rho\varphi_{\frac{k}{2}+i}(t) + \frac{\rho\theta'}{\rho-1} \times \left(-\alpha_i(t) + \alpha_{\frac{k}{2}+i}(t)\right)\right]. \tag{7c}$$

The amplitude and phase terms of the Σ-port and Δ-port are represented by α_Σ, φ_Σ, α_Δ, and φ_Δ, respectively. From (6) and (7), we can express the corresponding PSDs of the amplitude and phase fluctuations represented by S_{α_Σ}, S_{φ_Σ}, S_{α_Δ}, and S_{φ_Δ} as

$$S_{\alpha_\Sigma}(f) = \frac{2(1+\rho^2)}{k(1+\rho)^2}\left[S_\alpha(f) + \frac{2\rho^2\theta'^2}{(1+\rho)^2(1+\rho^2)}S_\varphi(f)\right] \tag{8a}$$

$$S_{\varphi_\Sigma}(f) = \frac{2(1+\rho^2)}{k(1+\rho)^2}\left[S_\varphi(f) + \frac{2\rho^2\theta'^2}{(1+\rho)^2(1+\rho^2)}S_\alpha(f)\right] \tag{8b}$$

$$S_{\alpha_\Delta}(f) = \frac{2(1+\rho^2)}{k(1-\rho)^2}\left[S_\alpha(f) + \frac{2\rho^2\theta'^2}{(1-\rho)^2(1+\rho^2)}S_\varphi(f)\right] \tag{9a}$$

$$S_{\varphi_\Delta}(f) = \frac{2(1+\rho^2)}{k(1-\rho)^2}\left[S_\varphi(f) + \frac{2\rho^2\theta'^2}{(1-\rho)^2(1+\rho^2)}S_\alpha(f)\right]. \tag{9b}$$

In (8) and (9), S_α and S_φ refer to the amplitude and phase noise of a single oscillator, respectively.

In the case of imperfect phase alignment ($\theta' \neq 0$), amplitude noise is projected to the phase quadrant, as indicated by the second term in (8). Similarly, a mapping of phase to amplitude also occurs. An expression for determining the angle that generates a specific PM-to-AM or AM-to-PM conversion can be obtained by taking the ratio between the first and second terms in (8). The phase alignment angles for the Σ-port and Δ-port are, respectively, given by

$$\theta'_\Sigma = \sqrt{\frac{(1+\rho^2)(1+\rho)^2}{2\beta\rho^2}} \tag{10a}$$

$$\theta'_\Delta = \sqrt{\frac{(1+\rho^2)(1-\rho)^2}{2\beta\rho^2}}. \tag{10b}$$

Here, β is the ratio of the noise PSDs; it is equal to S_φ/S_α for PM-to-AM conversion and equal to S_α/S_φ for AM-to-PM. Upon analyzing (10), it can be observed that the alignment angle for PM-to-AM conversion becomes significantly stricter at the Δ-port when compared with the Σ-port. Next, we discuss the implications of this on the output signals of the hybrid.

1) Σ—Port: The PPO output is available for the user at the Σ-port and is described by (6) and (8). For our oscillators, the PM noise is at least 30 dB higher than the AM noise for some carrier and offset frequencies. For example, at 100 MHz the PM noise of our PPO configuration is $\sim$−100 dBc/Hz and the AM noise is −140 dBc/Hz at 1-Hz offset frequency. Ideally, this implies that we require 50 dB of suppression between the PM and AM. For $\rho = 0.94$ and $\beta = 50$ dB, the equation (10a) requires phase alignment to be $\leq$0.4° to minimize the effect of PM-to-AM conversion.

2) Δ-Port: A carrier-suppressed signal for the noise measurement is present at the Δ-port and is described by (7) and (9). The PM-to-AM conversion is larger at this port, and this requires tighter phase alignment for a given β relative to the Σ-port. For a configuration of $\rho = 0.94$ and $\beta = 50$ dB, (10b) requires phase alignment for the carrier-suppressed signal to be within 11 millidegrees to minimize PM-AM conversion. This indicates that the phase alignment requirements for the CS signals at the Δ-port are $\approx$32 times more stringent compared with that for the signals at the Σ-port.

However, it is important to note that when oscillators are phased-locked to a common reference signal, the phase noise within the PLL BW is correlated, and therefore, it is also suppressed when a CS method is used. As a result, the need for high PM-to-AM rejection is relaxed within the loop BW. In our 100-MHz oscillator, the noise suppression inside the PLL BW is 15 dB, and taking this into account, the actual maximal amount of β needed is 35 dB. This corresponds to an

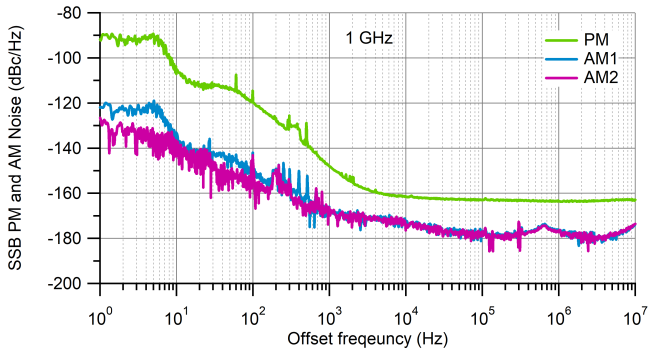

Fig. 3. PM and AM noise of 2-PPOs at 1 GHz measured using CS method. It shows the effect of PM-to-AM due to phase misalignment between two output signals when they are summed. AM1—phase alignment not optimized and AM2—phase alignment optimized.

alignment angle of ≈63 millidegrees, reducing the requirement by a factor of almost 6.

The strict phase alignment requirements during CS measurements were difficult to achieve and maintain with manual phase shifters, especially at 1 GHz. Fig. 3 illustrates the measured PM and AM noise of the 2-PPOs at 1 GHz. The plot displays the PM and AM curves for two different phase alignment cases. Below a 100-Hz offset, it is apparent that PM (green curve) noise is projected onto the AM (blue curve—AM1) noise due to misalignment in the summed signals. However, after proper phase alignment, this effect is reduced, as indicated by curve AM2 in magenta.

B. Noise Enhancement Factor (η)

In the experimental setup, it is difficult to measure the parameter ρ directly, so we can use other indirect measurements to determine it. Moreover, while (8) and (9) are instructive for analysis, they are not convenient for practical measurement purposes. For these reasons, we define a new parameter η, as the ratio of the power measured at Σ-port (P_Σ) relative to Δ-port (P_Δ)

$$\eta = \frac{(1+\rho)^2}{(1-\rho)^2} = \frac{P_\Sigma}{P_\Delta}. \tag{11}$$

The signal powers P_Σ and P_Δ are readily accessible and can accurately be measured. When the CS measurement technique is implemented, the AM and PM noise measured at Δ-port also increase by the factor, η, and this effectively improves the measurement system floor by the same amount. All the noise measurements made at the Δ-port must be divided by η to recover the actual noise of the device under test as if it were measured at the Σ-port without CS

$$S_{\Sigma\text{-port}} = \frac{S_{\Delta\text{-port}}}{\eta}. \tag{12}$$

This relationship is applicable to both AM and PM measurements. Furthermore, using (10b) and (11), one can rewrite alignment angle in terms of η as

$$\theta'_\Delta = \frac{2\sqrt{\frac{(\eta+1)}{\beta}}}{\eta - 1}. \tag{13}$$

C. Phase Alignment Using Digital Armstrong Modulator

To achieve phase alignment of the individual oscillator inputs to the power summer, we use a pure PM tone generated through a digitally modified version of an Armstrong-type modulator [29], [30]. This modulator is constructed using a direct digital synthesizer (DDS) clocked by oscillator #1 (OSC1 in Fig. 1). The DDS output is configured to produce a suppressed-carrier double-sideband (DSB-SC) modulation with a center frequency matching oscillator #1 and a 10-kHz modulation frequency. The DSB-SC signal is then combined with the output of oscillator #1 using a 20-dB DC acting as an injector. By adjusting the digital phase of the DDS carrier, we can control the AM-to-PM balance of the Armstrong modulator. This modulator is simpler compared with the I/Q mixer-based Armstrong modulator [31].

We meticulously align the phase of all the summed input oscillators by minimizing the PM-to-AM conversion of a pure PM tone using the following technique.

1) Initially, only oscillator #1 and the DSB-SC signal from the DDS are enabled.
2) The AM and PM components generated by the DSB-SC signal and oscillator #1 are monitored at the output hybrid (Δ-port) using a noise analyzer. The carrier phase of the DSB-SC signal is adjusted digitally on the DDS until a pure PM tone is achieved, indicated by an AM suppression greater than 40 dB relative to PM.
3) In addition to oscillator #1, oscillator #2 is enabled. Any phase misalignment of oscillator #2 will result in spurious AM in the power summed output. The phase shift of oscillator #2 is adjusted by introducing variable cable lengths for coarse control and using analog phase shifter #1 (φ_1 in Fig. 2) for fine-tuning. The phase shift is iteratively adjusted until the amount of spurious AM at the hybrid output is minimized.
4) The previous step is repeated four more times, individually aligning oscillators #3, #4, #5, and #6 with oscillator #1.
5) Finally, all the six oscillator outputs are enabled, and any detected spurious AM tone is minimized using analog phase shifter #2 (φ_2 in Fig. 1).

Since the DDS is limited to an output frequency of less than 160 MHz, when working with a 1-GHz carrier, we use two higher frequency synthesizers and a power summer to generate the DSB-SC signal.

V. Results

The SSB PM and AM noise characteristics of both a single oscillator and 6-PPOs at three different carrier frequencies are illustrated in Figs. 4–6, respectively. For 6-PPOs, at the Σ-port of the hybrid, the total power measured approximately +14, +17, and +13 dBm, and at the Δ-port, the CS power measured approximately equal to −32, −11, and −18 dBm for frequencies of 10, 100 MHz, and 1 GHz, respectively. The large variations in power levels at the Δ-port for different measurement configurations are due to the use of fixed value attenuators instead of variable attenuators to match power levels at the two input ports of the hybrid.

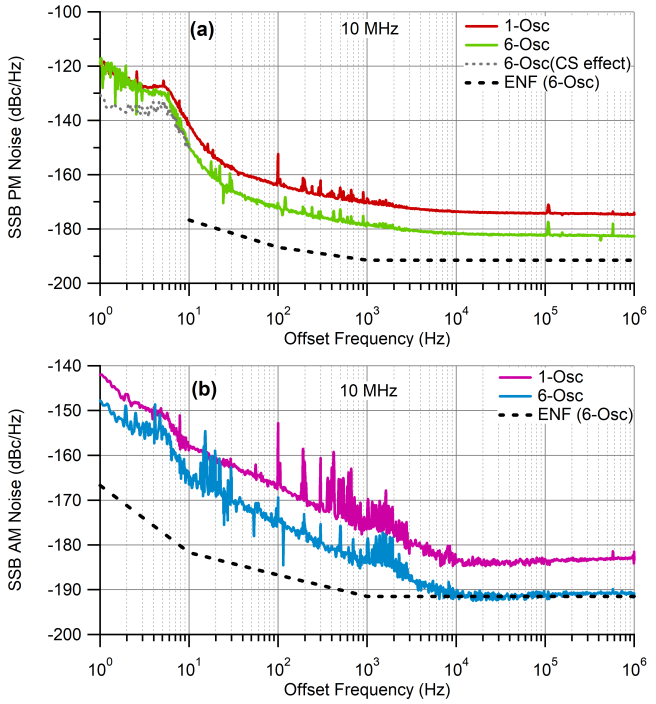

Fig. 4. SSB noise of single and multiple oscillators at 10 MHz. (a) PM noise. (b) AM noise. CS–carrier suppression; and ENF—effective noise floor.

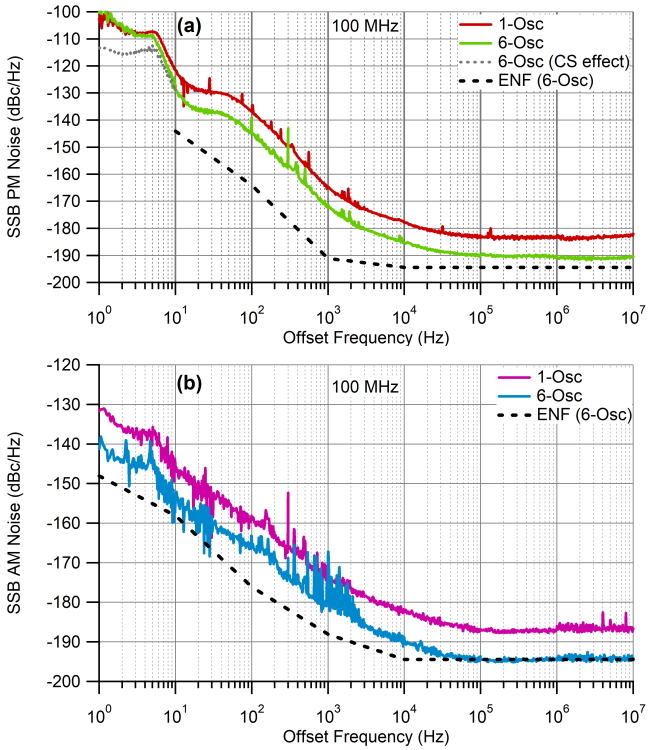

Fig. 5. SSB noise of single and multiple oscillators at 100 MHz. (a) PM noise. (b) AM noise. CS–carrier suppression; and ENF—effective noise floor.

For the six-oscillator configuration, the AM and PM noise were obtained from a pair of triplets of oscillators. The amplitude and phase of the pair were adjusted to produce a carrier-suppressed signal, and finally, the measured noise was scaled by η as described in (12) to obtain the PM and AM noise as it would be present at the Σ-port. This is valid because the independent noise powers of all the six oscillators add the same way for both Δ- and Σ-port signals. Similarly, for single oscillator, the PM noise and AM noise were obtained by measuring the CS signal at the delta-port generated from a 2-PPOs configuration (OSC1 and OSC4). In this case, the measured noise was scaled to that of a single oscillator by $\eta/2$, and an assumption was made that both the oscillators have equal noise.

The white noise floors for the 6-PPOs were estimated from scaled (η) thermal noise limits for the suppressed carrier power levels, and the close-to-the-carrier floors were obtained either from scaled (η) FSWP50 specifications or direct measurements.

It is important to consider several factors when interpreting the results of the PM and AM noise measurements.

For PM noise, since all the six oscillators in the array are phase-locked to a common 10-MHz reference oscillator, the phase noise measured with the CS technique is effectively suppressed below the locking BW (~6 Hz). Consequently, for all the three carrier frequencies, the absolute phase noise below the 10-Hz offset is measured without CS, while above the 10-Hz offset, the CS method is used. The final reported phase noise is a spliced plot of these two methods. The impact of the PLL when CS is used is depicted as a light gray dotted line in Figs. 4(a)–6(a).

For AM noise, the CS method is used for all the offset frequencies, since AM noise remains unaffected by the PLL. The AM noise of a single and multiple configurations is shown in Figs. 4(b)–6(b). For all the three carrier frequencies, the close-to-the-carrier AM noise displays a slope steeper than $1/f$, indicating the presence of PM-to-AM conversion that affects both single- and multiple-oscillator measurements. However, a notable improvement of approximately 7.8 dB in AM noise is observed, particularly at higher offset frequencies. This number matches the improvement given by theory; in fact, we expect an improvement of $10\log_{10}(k)$ dB, where k is the total number of oscillators in the array.

Maintaining phase alignment and CS greater than 30 dB over an extended period without automatic control proves challenging due to temperature variations. This difficulty is especially pronounced at 1 GHz when attempting to align all the six oscillators. In our experiment, imperfect alignment resulted in the AM of a single oscillator being lower than that of the multiple oscillators for a 1-GHz carrier at low offset frequencies.

Despite the challenges associated with phase alignment and the high level of PM-to-AM conversion observed in the AM case, the performance of phase-coherent array of oscillators yielded flicker AM noise levels of -148, -140, and -120 dBc/Hz at a 1-Hz offset for carrier frequencies of 10, 100 MHz, and 1 GHz, respectively. In addition, white AM noise levels below -182 dBc/Hz were achieved for all the three carrier frequencies.

Regarding the PM case, given that the AM noise was lower than the PM noise, the AM-to-PM conversion effect was

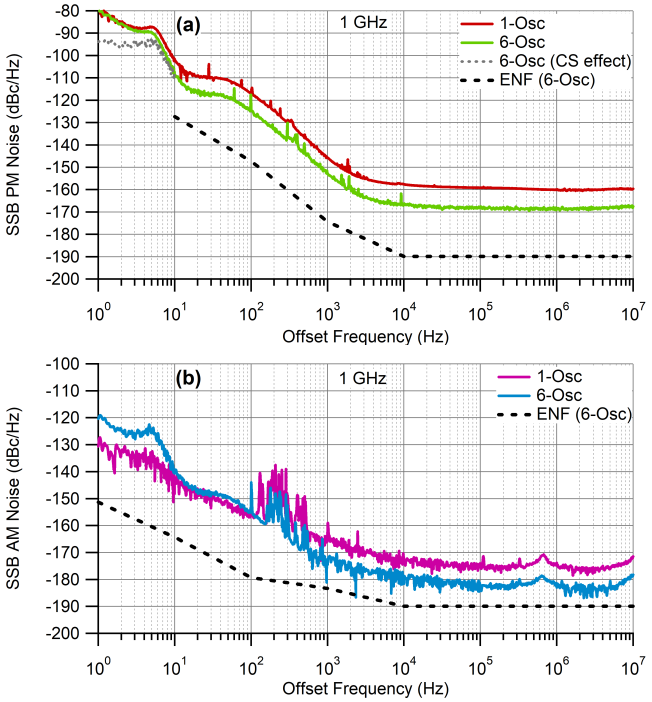

Fig. 6. SSB noise of single and multiple oscillators at 1 GHz. (a) PM noise. (b) AM noise. CS—carrier suppression; and ENF—effective noise floor.

negligible, and the phase alignment between different summing signals was not as critical. An improvement of approximately 7.8 dB was observed at all the offset frequencies outside the PLL BW for all the three carrier frequencies, reaching an impressive white noise levels of −182 dBc/Hz for 10 MHz, −191 dBc/Hz for 100 MHz, and −168 dBc/Hz for 1-GHz carrier frequencies.

It is also interesting to note that the 10- and 100-MHz oscillators used in this experiment exhibit AM noise at the thermal signal-to-noise limit, whereas their PM noise does not.

VI. Conclusion

In this study, we demonstrated that summing of multiple phase-coherent oscillators in a star configuration improves spectral purity by an amount that matches the theoretical value of $10\log_{10}(k)$ dB. However, it is crucial to ensure proper phase alignment of the oscillators to avoid unwanted AM-to-PM and PM-to-AM conversions in the combined output signal.

We constructed an array of six PPOs, where each oscillator could selectively produce one of the three different frequencies and was phase-locked to a common reference. By carefully aligning the phases, we achieved extremely low SSB white PM noise levels of −182, −191, and −168 dBc/Hz for 10, 100 MHz, and 1 GHz, respectively. Similarly, the white AM noise levels were approximately −191, −194, and −182 dBc/Hz. These noise levels, as anticipated for a configuration with six oscillators, exhibited an approximate 7.8-dB reduction compared with a single oscillator. However, due to PM-to-AM conversion, the AM noise near the carrier did not reach the theoretical 7.8-dB improvement. Implementing phase-locking with adjustable offset and phase detection at the summation point would allow for better control of the phase alignment over environmental variations and reduce PM-to-AM conversion. Nevertheless, at 10 MHz, the PM and AM noise levels at high-offset frequencies outperformed our previously reported results [32], [33]. We also observed that the 10- and 100-MHz oscillators show AM noise at the thermal signal-to-noise limit, whereas their PM noise does not.

Furthermore, we proposed a novel digital AM/PM modulator that simplifies the optimization of phase alignment and minimizes PM-to-AM and AM-to-PM conversion in arrayed configurations. This modulator can be readily used in analog single-channel and two-channel cross-spectrum PM noise measurements [34] to mitigate AM-to-PM conversion in the phase detectors.

Acknowledgment

The authors would like to thank David Howe, Nicholas Nardelli, Matthew Hummon, and anonymous reviewers for their constructive and useful comments on this article. Certain equipment, instruments, software, or materials are identified in this article to specify the experimental procedure adequately. Such identification is not intended to imply recommendation or endorsement of any product or service by NIST, nor is it intended to imply that the materials or equipment identified are necessarily the best available for the purpose.

References

[1] M. A. Richards, J. A. Scheer, and W. A. Holm, *Principles of Modern Radar: Basic Principles*. Rijeka, Croatia: SciTech, May 2010.

[2] G. L. Charvat, *Small and Short-Range Radar Systems*, 1st ed. Boca Raton, FL, USA: CRC Press, Apr. 2014.

[3] J. R. Vig, "Military applications of high accuracy frequency standards and clocks," *IEEE Trans. Ultrason., Ferroelectr., Freq. Control*, vol. 40, no. 5, pp. 522–527, Sep. 1993.

[4] M. R. Khanzadi, D. Kuylenstierna, A. Panahi, T. Eriksson, and H. Zirath, "Calculation of the performance of communication systems from measured oscillator phase noise," *IEEE Trans. Circuits Syst. I, Reg. Papers*, vol. 61, no. 5, pp. 1553–1565, May 2014.

[5] A. Piemontese, G. Colavolpe, and T. Eriksson, "Phase noise in communication systems: From measures to models," 2021, *arXiv:2104.07264*.

[6] T. Weber et al., "Noise in X-ray grating-based phase-contrast imaging," *Medical Phys.*, vol. 38, no. 7, pp. 4133–4140, Jul. 2011.

[7] D. Kang, "Effect of noise on modulation amplitude and phase in frequency-domain diffusive imaging," *J. Biomed. Opt.*, vol. 17, no. 1, Jan. 2012, Art. no. 016010. [Online]. Available: https://www.ncbi.nlm.nih.gov/pmc/articles/PMC4098065/

[8] A. Hati and C. W. Nelson, "*W*-band vibrometer for noncontact thermoacoustic imaging," *IEEE Trans. Ultrason., Ferroelectr., Freq. Control*, vol. 66, no. 9, pp. 1536–1539, Sep. 2019.

[9] D. T. Wymer, K. P. Patel, W. F. Burke, and V. K. Bhatia, "Phase-contrast MRI: Physics, techniques, and clinical applications," *RadioGraphics*, vol. 40, no. 1, pp. 122–140, Jan. 2020. [Online]. Available: https://pubs.rsna.org/doi/10.1148/rg.2020190039

[10] N. V. Nardelli et al., "10 GHz generation with ultra-low phase noise via the transfer oscillator technique," *APL Photon.*, vol. 7, no. 2, Feb. 2022, Art. no. 026105, doi: 10.1063/5.0073843.

[11] C. E. Calosso, A. C. Cárdenas Olaya, and E. Rubiola, "Phase-noise and amplitude-noise measurement of DACs and DDSs," *IEEE Trans. Ultrason., Ferroelectr., Freq. Control*, vol. 67, no. 2, pp. 431–439, Feb. 2020.

[12] G. Cibiel, M. Regis, E. Tournier, and O. Llopis, "AM noise impact on low level phase noise measurements," *IEEE Trans. Ultrason., Ferroelectr., Freq. Control*, vol. 49, no. 6, pp. 784–788, Jun. 2002.

[13] C. McNeilage, E. N. Ivanov, P. R. Stockwell, and J. H. Searls, "Review of feedback and feedforward noise reduction techniques," in *Proc. IEEE Int. Freq. Control Symp.*, May 1998, pp. 146–155.

[14] U. Rohde and A. Poddar, "Noise minimization techniques for RF and MW signal sources," *Microw. J.*, vol. 50, no. 9, pp. 136–162, Sep. 2007. [Online]. Available: https://www.microwavejournal.com/articles/5307-noise-minimization-techniques-for-RF-and-mw-signal-sources

[15] A. Chenakin, "Phase noise reduction in microwave oscillators," *Microw. J.*, vol. 52, no. 10, pp. 124–140, Oct. 2009. [Online]. Available: https://www.microwavejournal.com/articles/8625-phase-noise-reduction-in-microwave-oscillators

[16] R. Boudot and E. Rubiola, "Phase noise in RF and microwave amplifiers," *IEEE Trans. Ultrason., Ferroelectr., Freq. Control*, vol. 59, no. 12, pp. 2613–2624, Dec. 2012.

[17] K. Takagi, S. Serikawa, and T. Doi, "A method to reduce the phase noise in bipolar transistor circuits," *IEEE Trans. Circuits Syst. II, Analog Digit. Signal Process.*, vol. 45, no. 11, pp. 1505–1507, Nov. 1998.

[18] K. Takagi, S. Serikawa, and A. Okuno, "$1/f$ phase noise in a transistor and its application to reduce the frequency fluctuation in an oscillator," *Microelectron. Rel.*, vol. 40, no. 11, pp. 1943–1950, Nov. 2000.

[19] A. Hati, C. W. Nelson, and D. A. Howe, "Oscillator PM noise reduction from correlated AM noise," *IEEE Trans. Ultrason., Ferroelectr., Freq. Control*, vol. 63, no. 3, pp. 463–469, Mar. 2016.

[20] Y. Okabe and S. Okamura, "Analysis of the stability and noise of oscillators in free, synchronized, and parallel running modes," *Elect. Commun. Jpn.*, vol. 52-B, no. 12, pp. 102–110, 1969.

[21] M. M. Driscoll, "A SAWR oscillator vibration sensitivity and phase noise reduction technique using multiple resonators and RF outputs," in *Proc. IEEE Ultrason. Symp. (ULTSYM)*, May 1994, pp. 514–518.

[22] H.-C. Chang, X. Cao, U. K. Mishra, and R. A. York, "Phase noise in coupled oscillators: Theory and experiment," *IEEE Trans. Microw. Theory Techn.*, vol. 45, no. 5, pp. 604–615, May 1997.

[23] P. Maffezzoni, B. Bahr, Z. Zhang, and L. Daniel, "Reducing phase noise in multi-phase oscillators," *IEEE Trans. Circuits Syst. I, Reg. Papers*, vol. 63, no. 3, pp. 379–388, Mar. 2016.

[24] K. H. Sann, "The measurement of near-carrier noise in microwave amplifiers," *IEEE Trans. Microw. Theory Techn.*, vol. MTT-16, no. 9, pp. 761–766, Sep. 1968.

[25] E. N. Ivanov, M. E. Tobar, and R. A. Woode, "Microwave interferometry: Application to precision measurements and noise reduction techniques," *IEEE Trans. Ultrason., Ferroelectr., Freq. Control*, vol. 45, no. 6, pp. 1526–1536, Nov. 1998.

[26] C. W. Nelson, A. Hati, and D. A. Howe, "Phase inversion and collapse of cross-spectral function," *Electron. Lett.*, vol. 49, no. 25, pp. 1640–1641, Dec. 2013. [Online]. Available: https://onlinelibrary.wiley.com/doi/abs/10.1049/el.2013.3022

[27] A. Hati, C. W. Nelson, and D. A. Howe, "Cross-spectrum measurement of thermal-noise limited oscillators," *Rev. Scientific Instrum.*, vol. 87, no. 3, Mar. 2016, Art. no. 034708, doi: 10.1063/1.4944808.

[28] Y. Gruson, A. Rus, U. L. Rohde, A. Roth, and E. Rubiola, "Artifacts and errors in cross-spectrum phase noise measurements," *Metrologia*, vol. 57, no. 5, Aug. 2020, Art. no. 055010, doi: 10.1088/1681-7575/ab8d7b.

[29] E. H. Armstrong, "A method of reducing disturbances in radio signaling by a system of frequency modulation," *Proc. IEEE*, vol. 72, no. 8, pp. 1042–1062, May 1984.

[30] E. N. Ivanov, "Generation of pure phase and amplitude-modulated signals at microwave frequencies," *Rev. Scientific Instrum.*, vol. 83, no. 6, Jun. 2012, Art. no. 064705. [Online]. Available: http://rsi.aip.org/resource/1/rsinak/v83/i6/p064705_s1

[31] A. Hati and C. W. Nelson, "A simple optimization method for generating high-purity amplitude and phase modulation," *IEEE Trans. Instrum. Meas.*, vol. 71, pp. 1–9, 2022.

[32] A. Hati et al., "State-of-the-art RF signal generation from optical frequency division," *IEEE Trans. Ultrason., Ferroelectr., Freq. Control*, vol. 60, no. 9, pp. 1796–1803, Sep. 2013.

[33] M. Pomponio, A. Hati, and C. Nelson, "Ultra-low phase noise frequency division with array of direct digital synthesizers," *IEEE Trans. Instrum. Meas.*, early access, Dec. 25, 2023, doi: 10.1109/TIM.2023.3346538.

[34] W. Walls, "Cross-correlation phase noise measurements," in *Proc. 46th. IEEE Freq. Control Symp.*, May 1992, pp. 257–261, doi: 10.1109/FREQ.1992.270007.

Archita Hati (Member, IEEE) is an Electronics Engineer with the Time and Frequency Division, National Institute of Standards and Technology, Boulder, CO, USA, where she is the Calibration Service Leader of the Phase Noise Metrology Group. She is also an Associate Editor of IEEE TRANSACTIONS ON ULTRASONICS, FERROELECTRICS, AND FREQUENCY CONTROL, since 2021. Her research interests include phase noise metrology, ultralow-noise frequency synthesis, development of low-noise microwave and opto-electronic oscillators, and vibration analysis.

Dr. Hati was a recipient of the Allen V. Astin Measurement Science Award "For developing a world-leading program of phase noise research and measurement services to support industry and national priorities," in 2015.

Marco Pomponio received the M.Sc. degree in electronic engineering from the Polytechnic of Turin in collaboration with the Italian National Metrology Institute (INRIM), Turin, Italy, in 2017. He is currently pursuing the Ph.D. degree with the Colorado University of Boulder in collaboration with the National Institute of Standards and Technology (NIST), Boulder, CO, USA. In 2018, he presented the M.Sc. thesis work at the European Frequency and Time Forum (EFTF), where he won the student poster competition, and he won the same competition again, in 2021.

He is an Electronics Engineer at the Colorado University of Boulder in collaboration with the National Institute of Standards and Technology (NIST). He has been working as a Research Assistant with NIST, since 2018. His research fields include high-performance digital control loops, field-programmable gate arrays (FPGAs), signal processing, low-noise electronics and phase, and amplitude noise metrology.

Craig W. Nelson (Member, IEEE) is an Electrical Engineer and Leader of the Phase Noise Metrology Group at the National Institute of Standards and Technology (NIST), Boulder, CO, USA. His involvement in this group spans over three decades, and research interests include phase and amplitude noise metrology, low-noise electronics, FPGA-based digital control, and instrument control. He has authored more than 70 articles and teaches classes, tutorials, and workshops at NIST, the IEEE Frequency Control Symposium, and several sponsoring agencies on the practical aspects of high-resolution phase noise metrology.

Mr. Nelson was a recipient of the NIST Bronze Medal in 2012, the Allen V. Astin Measurement Science Award "For developing a world-leading program of phase noise research and measurement services to support industry and national priorities" in 2015, and the IEEE Cady Award "For leadership in the design and development of state-of-the-art low noise oscillators and phase noise measurement systems" in 2020.